Contributed Papers from Materials Science and Technology 2016 (MS&T16)
October 23 – 27, 2016, Salt Palace Convention Center, Salt Lake City, Utah USA

THE NOVEL USE OF ACOUSTIC EMISSION MONITORING DURING PROOF-TESTING OF CERAMIC SPINAL IMPLANTS

Darin A. Ray[*1], Ramaswamy Lakshminarayanan[†1], Bryan J. McEntire[1], and Obdulia Ley[2]

[1]Amedica Corporation, Salt Lake City, UT 84119
[2]MISTRAS Group, Inc., Princeton Junction, NJ 08550

Keywords: silicon nitride, acoustic emission, proof test, defects

Abstract

An added level of safety and reliability is required of implantable medical devices, particularly when they are prepared from brittle materials. For ceramics, proof-testing has been commonly employed as an inspection method to assure that devices meet minimum acceptance standards. However, proof-testing does not necessarily identify all latent defects. Consequently, subsequent visual inspection methods are employed to eliminate potentially flawed components. In this study, a novel approach of coupling acoustic emission (AE) monitoring with proof-testing was developed for silicon nitride (Si_3N_4) intervertebral spinal spacers in order to eliminate the need for subjective visual inspection. The characteristic difference in AE signals for defective and non-defective components was rationalized and validated. AE testing was able to identify defects which led to crack propagation during proof-testing. These types of defects would have otherwise remained undetected or required additional inspection using less reliable and more time-consuming techniques.

Introduction

Silicon nitride (Si_3N_4) is currently used as intervertebral spacers in spinal fusion surgery, and is being developed as a bearing material in total hip arthroplasty (THA) because of its favorable properties which include high strength, toughness, biocompatibility, osseointegration, bacteriostasis, improved imaging, hardness and wear resistance.[1–14] While demonstration of acceptable biocompatibility, mechanical properties and wear behavior are regulatory prerequisites for approval of implantable devices, the ongoing assurance that manufactured implants consistently satisfy safety and efficacy requirements rests primarily with the device manufacturer. Process validation and compliance with current good manufacturing practices (cGMP) are additional regulatory necessities ensuring the reliability of manufactured components.[15] However, further assurance is provided by subjecting components to 100% proof-testing, which is particularly critical for ceramics due to their stochastic brittle nature. Proof testing of ceramic components is a well-established technique used in a variety of settings to ensure that implants have sufficient strength for the intended application and that defective parts are rejected.[16–25] However, if failure is not readily apparent during proof testing, subjective additional examinations, such as magnified visual or fluorescent penetrant inspection

[*] Author to whom correspondence should be addressed. e-mail: dray@amedica.com
[†] Current address: Corning Inc., Sullivan Park Campus, Painted Post, NY 14870

(FPI), are required. These techniques check for defects or damage which may be present prior to, or occurring during proof testing. Unfortunately, these additional inspection steps have several limitations including those related to the defect itself (size and detectability), as well as environmental and operator factors such as lighting, visual acuity and inspector fatigue,[26,27] all of which result in a time consuming process subject to human error. To combat this deficiency, extensive operator training is employed to reduce inspection time while attempting to maximize detectability and minimize human error. Nevertheless, a finite risk of misidentifying defects remains due to the subjective nature of these inspection methods.

Non-destructive testing (NDT) or inspection (NDI) of ceramics using methods, such as ultrasonics, thermal imaging, x-ray computed tomography (CT), nuclear magnetic resonance (NMR) and other forms of radiography or spectroscopy, dye or fluorescent penetrant testing, are commonly employed for identifying defects without inducing damage to components.[28–30] These can be effective in detecting defects in less complex geometries, but are also time and labor intensive with subjective, operator dependent outcomes. Another NDT technique, acoustic emission (AE) testing, was suggested by Evans *et al*.[31] as a means of stress monitoring and failure prediction of ceramic parts. AE testing is a method particularly well-suited for identifying failures during proof testing.[25,32]

There are broadly three application areas for the AE technique: 1) structural testing and surveillance, 2) process monitoring and control, and 3) materials characterization.[33] The work performed in this paper falls within the structural (proof) testing and materials characterization areas. Today, the goals of acoustic emission examinations in industrial applications are: detection, location and assessment of flaws in structures. The structures or parts monitored can be made of various materials. AE has been widely used for in situ monitoring of damage development in metals,[34–36] composites, and ceramics.[37,38] AE signals are used to identify crack growth and propagation, as well as to establish pass-fail relationships of various material types and structures.[39–41] Collection and characterization of AE signals has been used for controlling various industrial processes, like grinding,[42] precision manufacturing or machining,[43,44] welding,[45] and tool quality.[46] In these applications, the correlation between acoustic emission signals and subsurface integrity is determined to analyze the progression of the processes and the workpiece quality.[47]

Application of acoustic emission as a diagnostic method, as part of a proof test or as a structural integrity assessment tool, is possible when a qualitative or quantitative relationship between the detected acoustic emission and material condition is established for a specific material and structure. There are two major approaches to achieve this goal: 1) Determining experimentally a characteristic set (fingerprints) of acoustic emission parameters and their characteristics that uniquely describe a material condition, fracture stage, flaw type, etc., and (2) Establishing a theoretical relationship between acoustic emission parameters and their characteristics and material properties, fracture mechanics parameters, etc. A summary of the work developing both approaches for various structures and materials is presented by Miller *et al*.[48]

Unlike other NDT techniques which rely on an external energy source (*i.e*., ultrasonic, X-rays, thermal, etc.) to interact with flaws, it is the defect itself in AE testing that acts as the source of excitation in response to an applied stress. In the case of proof testing ceramic spinal implants,

the stress is simply applied through mechanical means. Movement of a discontinuity, fracture development and crack jumps under static or dynamic loads are followed by a rapid release of energy which produces high frequency elastic waves (20KHz to 1MHz) traveling within the material. The acoustic emission technique uses one or more piezoelectric type sensors to detect these waves.

By monitoring acoustic emissions produced by the implant during proof testing, immediate feedback about new or existing damage in the implant is provided to the operator, and components can be directly accepted, rejected or subjected to further evaluation as may be necessary. Due to the capability of AE to detect crack initiation and propagation, as well as friction between existing crack surfaces, employment of AE testing is less subjective, and has the advantage of eliminating secondary NDT methods, including microscopic visual and fluorescent penetrant testing.

In this study we report on the development, validation and use of AE monitoring during proof testing of silicon nitride intervertebral spinal spacers. Crack propagation signals were collected from testing to failure and such characteristics were used to filter and differentiate crack propagation from friction. The combination of AE monitoring during mechanical loading of implants proved to be an effective approach to assuring their structural integrity, while concurrently reducing or eliminating subsequent subjective and labor intensive secondary inspection methods. Important general observations and considerations when using AE testing are presented and discussed.

Materials and Methods

Material and Component Production

Various silicon nitride interbody spinal spacers (Valeo^{TM}, AMEDICA Corp, Salt Lake City, UT) were manufactured using standard industry techniques to mix, consolidate and form Si_3N_4, yttrium oxide (Y_2O_3) and aluminum oxide (Al_2O_3) powders into compact green bodies. The material composition (6 wt.% Y_2O_3, 4 wt.% Al_2O_3, 90 wt.% Si_3N_4) and processing methods were reported previously,[3] and are similar to those discussed by Iturriza *et al*.[49] Following production of the implants, proof testing and acoustic emission monitoring were performed as outlined in Figure 1.

Proof Testing & AE Monitoring

Proof testing was conducted using a universal test machine (Model 5567, Instron, Norwood, MA) by applying compressive and shear loads to the implant through a polymeric fixture at a crosshead speed of 5 mm/min to a pre-determined proof test stress and unloaded at a crosshead speed of 20 mm/min. The proof testing apparatus with mounted AE sensors is shown in Figure 2. The applied proof test stress was determined as the mathematical product of the maximum expected *in vivo* stress and a nominal safety factor of 2.5. The maximum possible *in vivo* stress was conservatively estimated to be 15 MPa based on reported vertebral bone strengths.[50,51] At stresses above 15 MPa, the vertebral bone would be expected to fail resulting in subsidence of the implant into the vertebral endplate. Polypropylene spacers which deformed under the proof test load were placed in-between the steel loading fixture and implant in order to eliminate high contact stresses associated with point-loading, and to allow for a more uniformly distributed proof test load.

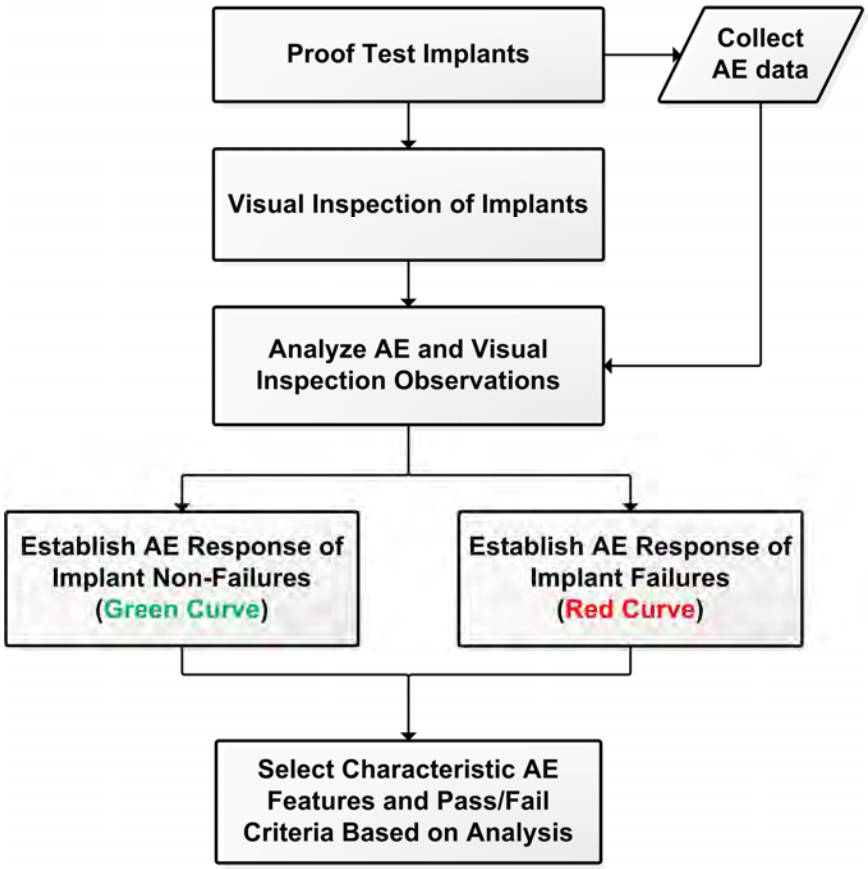

Figure 1. Primary steps for establishing acoustic emission monitoring as a method for identifying defects during proof testing.

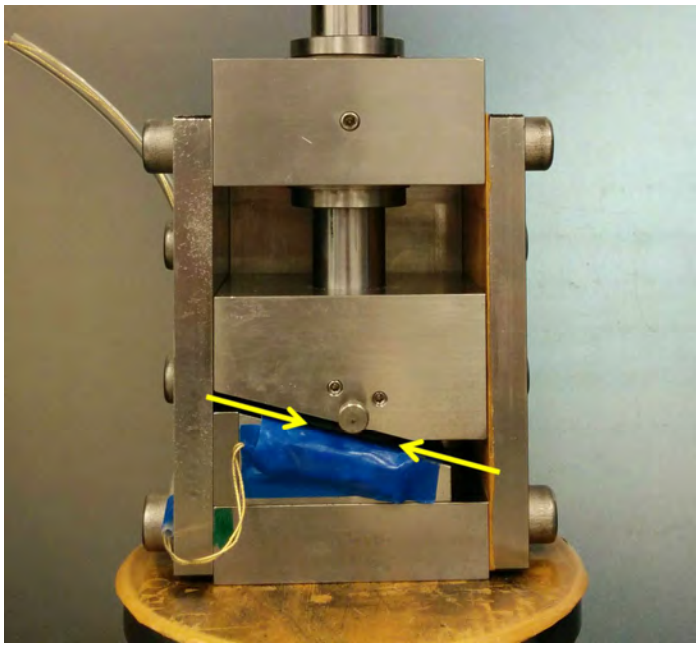

Figure 2. Proof testing apparatus instrumented with AE sensors. The mounted AE sensors are covered with protective tape to limit user contact. The implant (not visible) is positioned within the test apparatus, as indicated by the arrows.

Concurrent with performing the proof test, AE signals were collected using an acoustic emission system, external preamplifiers and 2 AE piezoelectric sensors with a resonant frequency of 300 kHz (MISTRAS Group Inc., Princeton Junction, NJ). The external AE preamplifiers were set to a gain of 40 dB with AE acquisition threshold of 35 dB, sampling rate of 2 million samples per second and bandpass filter of 100-3000 kHz. In some tests, where the AE hit amplitudes routinely exceeded the 100 dB limit of the sensors, the preamplifier on one of the two channels was set to a gain of 20 dB. Data acquisition at this lower preamp gain level (while leaving the software configuration set for the higher preamp setting) allowed for the high amplitude hits to effectively be shifted 20 dB lower and collected below the 100 dB limit. Data reported in this study are from a single channel at the 40 dB preamp gain setting unless stated otherwise.

Within the test set-up there were many sources of AE signals besides those originating from fracture of the ceramic implant. Frictional contact points between fixture and implant, or the associated friction of the proof testing apparatus itself acted as sources of AE signals. Interactions between the implant and fixture, fixture and test machine, other contacting/moving surfaces of the fixture and the mechanisms of the test machine (*i.e*., motor, ball screw-driven crosshead, etc.) all had the potential to be picked up by the AE system. Characterization of AE signals from these interactions is critical to the process and represents what is considered to be background noise. The AE sensor type and position was selected during a pilot testing phase to minimize these aberrant AE signals.

After set-up, calibration and pilot-testing to verify functionality, AE data were acquired on 542 standard production implants (Group 1), representing a broad range of shapes and sizes corresponding to their use in various locations within the cervical and thoracolumbar spine, and for different surgical approaches (*i.e*. anterior, posterior, transforaminal, etc.). These parts were subsequently visually inspected under magnification (10-30X). The visual observations associated with individual AE tests were used to identify false-positive events. This allowed for an assessment and construction of a background noise distribution for non-failure events, and for development of AE signal features (*e.g*. amplitude, energy counts and average frequency, etc.) associated with true failures.

Due to the extremely low proof test failure rate (<<1%) a large sample size would have been needed to collect enough AE data to fully characterize the AE signal features of failed implants. Because this was not a viable option, existing implant designs were modified (*i.e*. weakened) to consistently cause fractures at or below standard proof test stresses. Finite element analysis software (ANSYS, ANSYS, Inc., Canonsburg, PA) was used to evaluate several modified designs and determine those most likely to fail during proof testing. The modifications consisted of reduced implant wall thickness and/or reduced beam thicknesses on the implant fenestration features as illustrated in Figure 3. Subsequent testing confirmed that a significant percentage of these modified implants failed at or below proof test stresses. Proof tests and subsequent visual inspections under magnification (10-30X) were performed on 38 modified implants (Group 2). Visually observed failures were correlated with individual AE tests and signals. Implants that did not fail at standard proof test stresses were re-loaded to higher stresses until failure occurred, followed by visual inspection as before. AE signals from the failure of these modified implants were used to characterize the unique signals caused by crack propagation under the applied proof test stresses, and the outputs used to generate failure distribution plots.

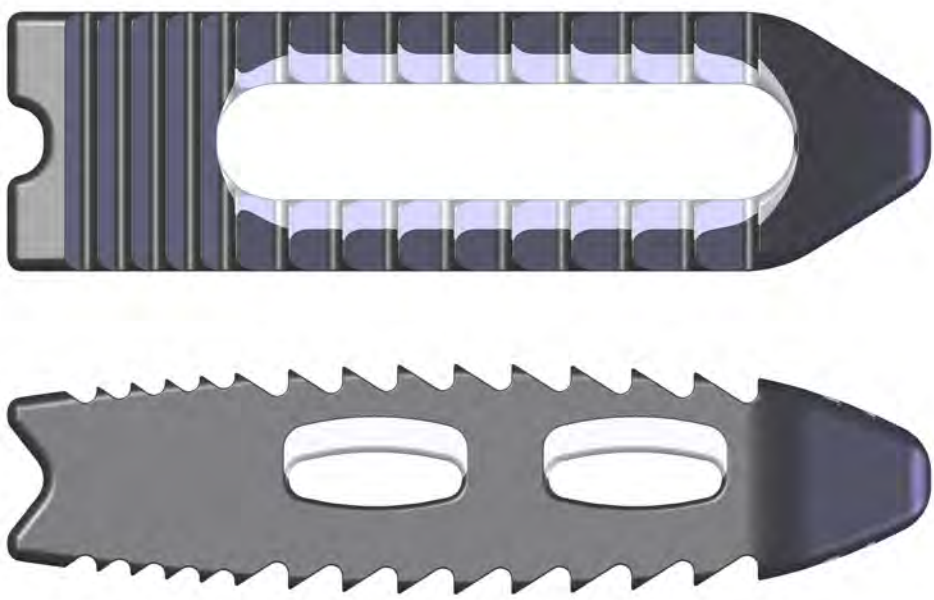

Figure 3. An example of modifications (reduced wall thickness and window beam thickness) made to implants to cause failure at or below standard proof test stresses shown in top and side views. Light areas represent material that was removed from the standard implant resulting in the weaker, modified implant (dark gray implant).

AE Data Analysis & Identification of Distinguishing AE Signal Features

Following proof testing and visual inspection, an analysis of the collected AE data was performed to understand the distribution of the various AE signal features including, among others, amplitude, energy counts and average frequency. To facilitate the analysis, some filters were used to eliminate hits that were clearly erroneous or extraneous. These filters rejected AE hits that (1) had average frequencies outside the principal operating range of the AE sensors (< 10.00 kHz and > 500.00 kHz), (2) were collected during handling, manual pre-loading and initial loading (≤ 500 N) of the implant, and (3) had very low energy counts (0-3 energy counts) which were considered insignificant.

Standard statistical methods and software (Minitab 15, Minitab Inc., State College, PA) were used to evaluate the collected AE data. The statistical methods used include Student's 2-sample t-tests and probability distribution plots at a significance level of $p \leq 0.05$.

Before collection and analysis of the data, it was uncertain how the data would be distributed, although it was hypothesized that there would be one or more AE signal feature, or combination of signal features that could be used to clearly differentiate between distributions for failures and non-failures. Pass/fail criteria were then selected based on a risk assessment of Type II (*i.e.*, accepting failed parts) and Type I (*i.e.*, rejecting non-failed parts) errors. Figure 4 shows the potential scenario of overlapping failure and non-failure distributions and pass/fail criterion. With the selected pass/fail criterion, the probabilities of Type I and II errors are represented by the areas under the respective curves. Based on the AE signal features of interest and the associated distributions, a biased pass/fail criteria was selected in favor of making Type I over Type II errors. While rejecting a good part is not desirable for economic reasons, it potentially carries less risk than accepting a bad part, which may have implications for device effectiveness

and patient safety. Pass/fail criteria were selected in light of these associated risks. The most desirable scenario is one in which the AE signal feature distributions are significantly differentiated and for which a pass/fail criterion can be selected such that the risks of both Type I and Type II errors are negligible or at levels acceptable for business and safety purposes, respectively. This particular scenario is presented in Figure 5.

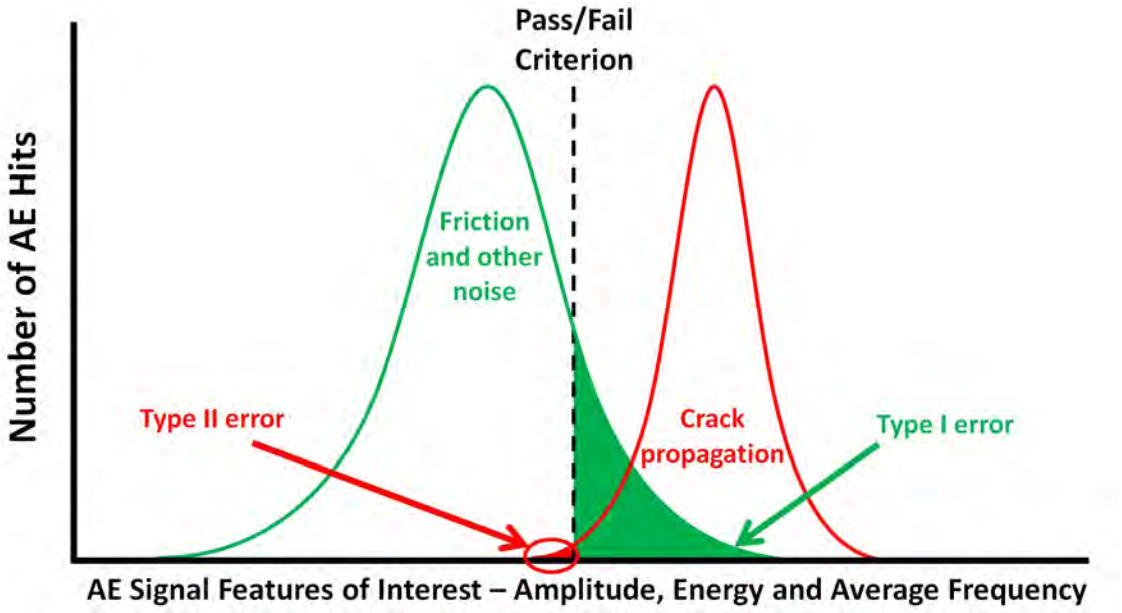

Figure 4. Potential distribution plots of AE hits versus various parameters of interest for failures and non-failures. A pass/fail criterion is identified as well as areas of Type I and Type II errors.

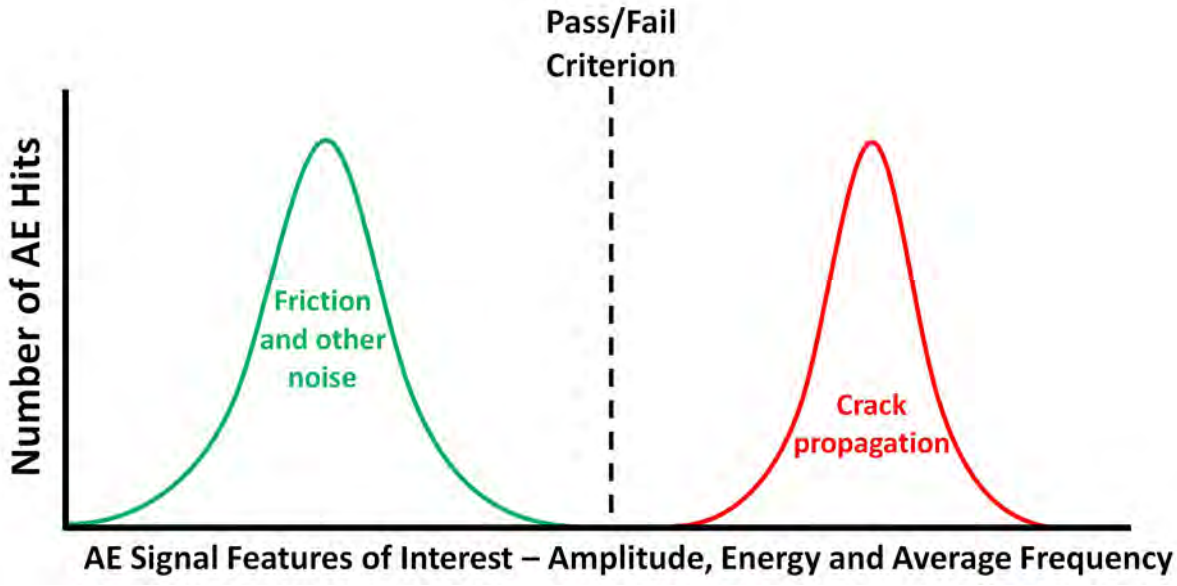

Figure 5. Potential distribution plots of AE hits versus various parameters of interest. The clear distinction between failures and non-failures and the selection of the pass/fail criterion can be used to minimize Type I and Type II errors.

It important to note that while data filters and AE equipment limitations (inability to collect some AE hits below or above a given threshold) resulted in the truncation of data distributions, the AE data analysis still represents an appropriately conservative approach. Namely, the mean values associated with non-failure distributions (Green Curves) are assumed to be greater than actual because most of the noise signals are filtered out or fall below the acquisition threshold. Similarly, the mean values associated with failure-distributions (Red Curves) are assumed to be less than actual because the sensors may have finite limits and, for example, may cut off hits with decibel values above the 100 dB maximum.

Results and Discussion

AE Data and Distributions of Standard Production Implants (Group 1) – Non-Failure Distributions (Green Curves)

Collection of AE data during proof testing of the 542 implants from 24 standard production lots was completed by multiple operators over the course of several days. Testing of Group 1 implants represented a wide range of device families, footprints and heights. A total of 45,163 AE hits were collected prior to any data filtering. The majority of hits occurred during loading and unloading of the implant from the proof test fixture by the operator. Sliding or slight movements of the fixture in and out of the universal test machine during this phase of the test resulted in a significant number of hits. Because there was no load applied during this period, the collected data were inconsequential. After removing this irrelevant data, there were 3,102 hits remaining. The average frequency and low energy count filters, as previously described, further reduced this total to 115 hits for the 542 tested implants. Detailed visual inspection under magnification (10-30X) identified no apparent fractures after proof testing. Because no failures were observed, the "Group 1" distributions and the "Green Curve" distributions are the same. The histogram plots (Figure 6 through Figure 8) were created from the filtered data and represent the non-failure (green curve) distributions. The histograms plot the percentage of hits as a function of the respective variable (*i.e*. average frequency, amplitude or energy) over defined intervals (shown on the plot as boxes/bins). A plot representing a normal distribution of the data is also shown.

AE Data and Distributions of Modified Implants (Group 2) – Failure Distributions (Red Curves)

AE data were then collected on 38 implants from four different modified implant designs. The specific modifications to wall and window beam thicknesses for each of the four groups are described in Table I. Standard proof testing resulted in fracture of 20 out of 38 implants (*cf*., Table I). Following standard proof testing, implants that did not fail were tested to greater loads until failure occurred. All remaining parts failed at or below ~1.54 times the standard proof test stress (*cf*., Table I). Overall, failures ranged from 0.70 to 1.54 times the standard proof test stress. Failures were observed under visual inspection (10-30X magnification) and appeared as fractures in the high stress areas of the implants as expected, and as previously identified by finite element analysis. Because "Group 2" implants were the only source of implant failures, the "Group 2" distributions and the "Red Curve" distributions are the same. AE monitoring collected a total of 5,964 hits prior to any filtering. Removal of data associated with loads less than 500 N resulted in 858 hits. Applying the average frequency and low energy count filters further reduced the number of hits to a total of 129. Analysis of data collected with the 40 dB preamp gain showed at least one 100 dB hit was observed for each of the 38 implants during fracture. This meant that the signals reached the maximum amplitude possible in this particular

hardware and software configuration. Taking the maximum amplitude hit for each implant resulted in a distribution that appeared to be a single value, because signals greater than 100 dB were truncated. These 38 hits (100 dB) were used to generate the red curve distributions in Figure 6 through Figure 8 for the AE signal amplitude, energy and average frequency, respectively. Note that in order to properly display the Group 2 "single value" distribution (100 dB) in Figure 6, two additional points were added to the data set at 99 and 101 dB. This results in a non-zero standard deviation, though it is was only performed to facilitate proper display of the distribution and the mean decibel value.

After observing that the sensor had recorded the maximum hit amplitude possible on the first 8 implants, one channel was changed to the 20 dB preamp gain setting and AE data was collected on the remaining 30 of 38 implants. The maximum amplitude hit from each of the 30 failure tests is presented in Figure 9. The AE hit amplitudes ranged between 85 and 95 dB with a mean and standard deviation of 93.5 ± 2.0 dB.

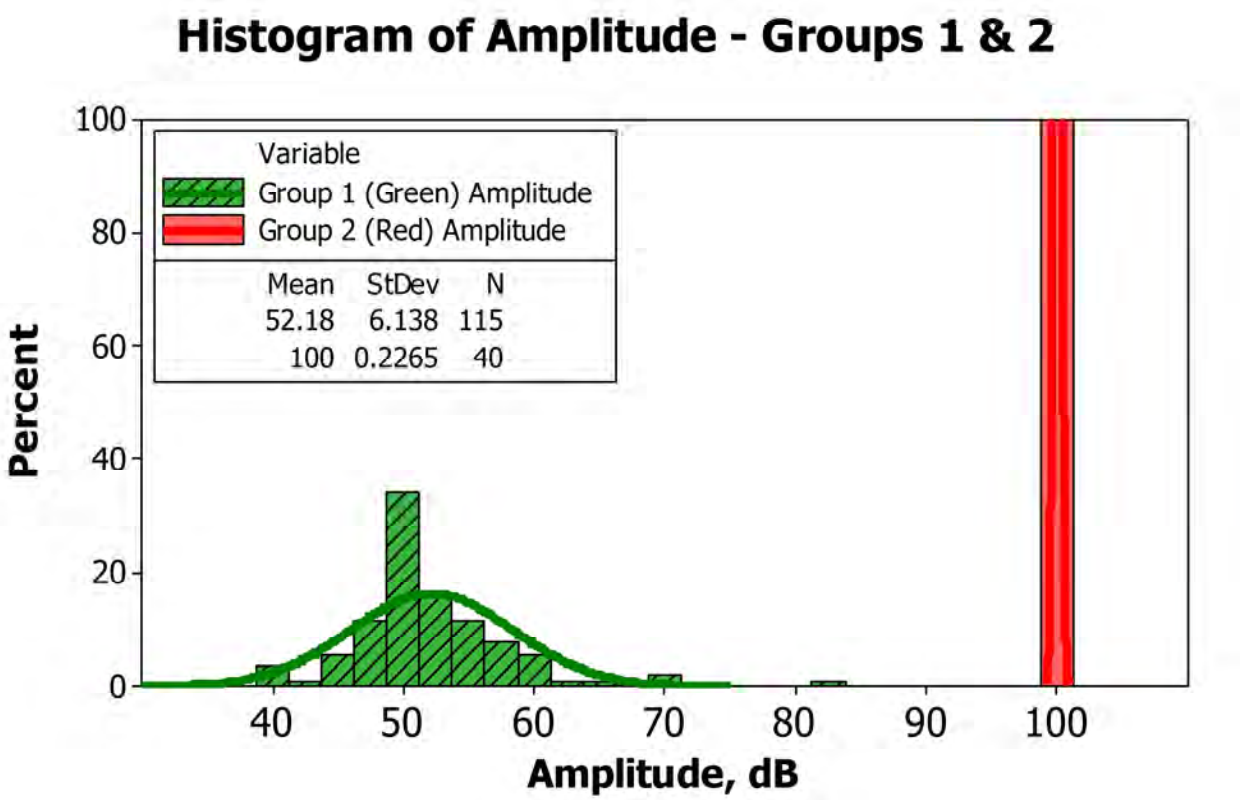

Figure 6. Distribution plot of AE hit amplitude for both Group 1 (Green) and Group 2 (Red) data.

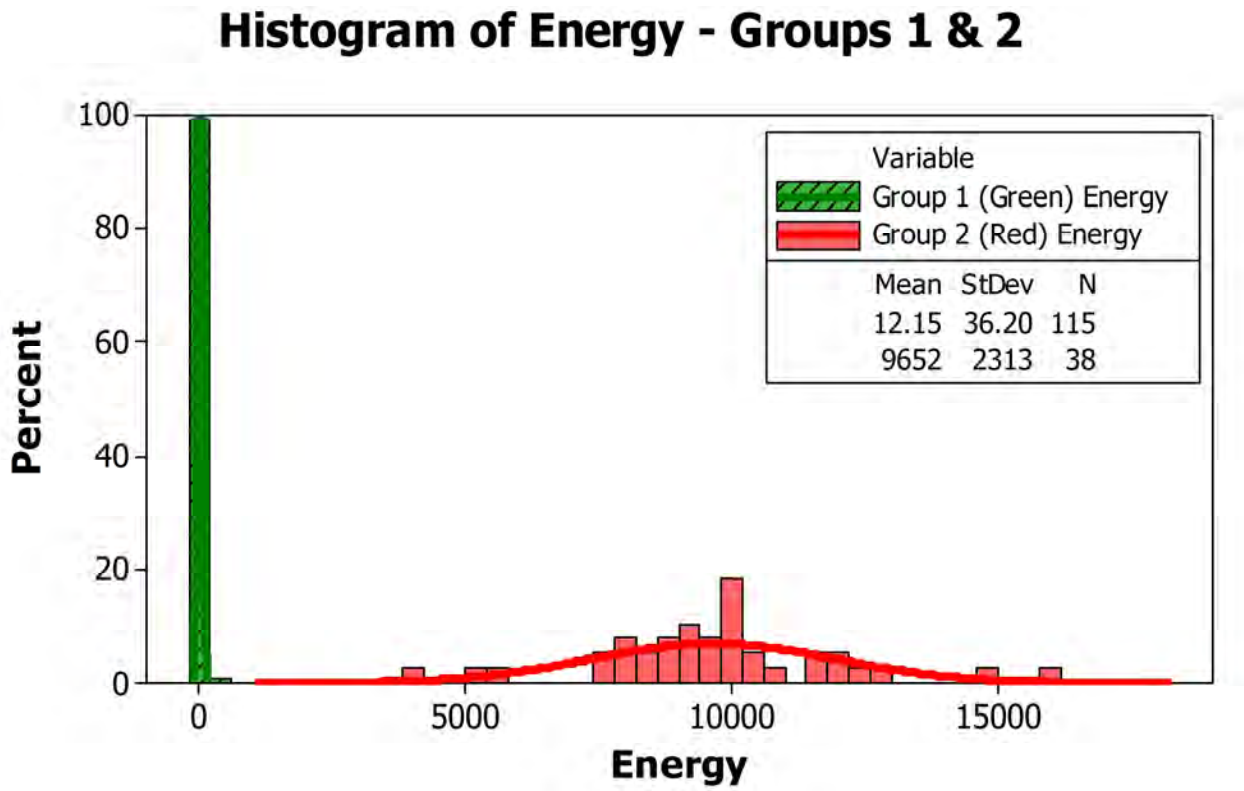

Figure 7. Distribution plot of AE hit energy for both Group 1 (Green) and Group 2 (Red) data.

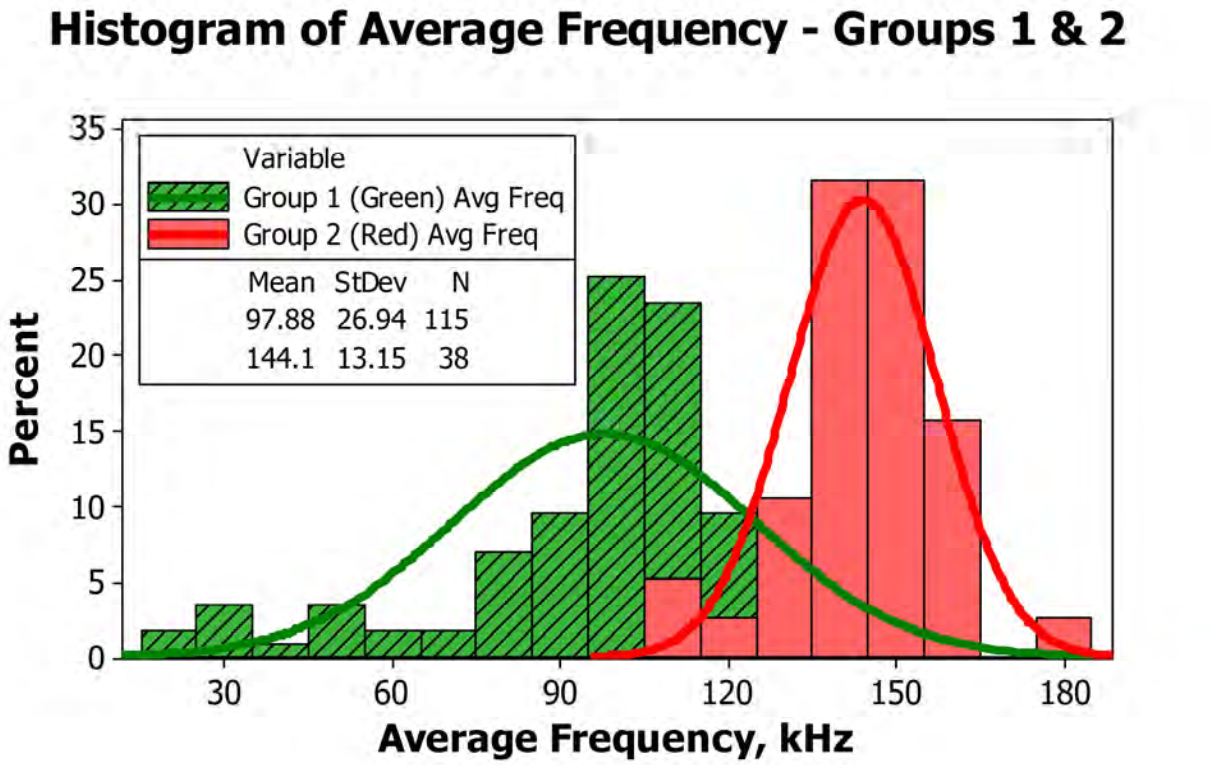

Figure 8. Distribution plot of AE hit average frequency for both Group 1 (Green) and Group 2 (Red) data.

Table I. Description and Test Details of Implants Used for Generation of Group 2 (Red) Distribution Curve.

Design	Implant Modifications		Total Qty	Max Applied Stress Factor[a]	Failure / Total Tested
	Bridge Thickness (mm)	Wall Thickness (mm)			
A	1.0 mm (top only)	1.5	9	1.00	8/9
				1.27	1/1[b]
B	1.0 mm (top only)	2.0	10	1.00	4/10
				1.27	6/6[b]
C	1.5 mm (top and bottom)	1.5	9	1.00	7/9
				1.27	2/2[b]
D	1.0 mm (top only)	2.5 (standard thickness)	10	1.00	1/10
				1.54	9/9[b]

a. Maximum applied stress expressed as a factor of the standard proof test stress. Failures occurred at or below this stress level.
b. Remaining implant(s) that did not fail at standard proof test stress and were retested to failure.

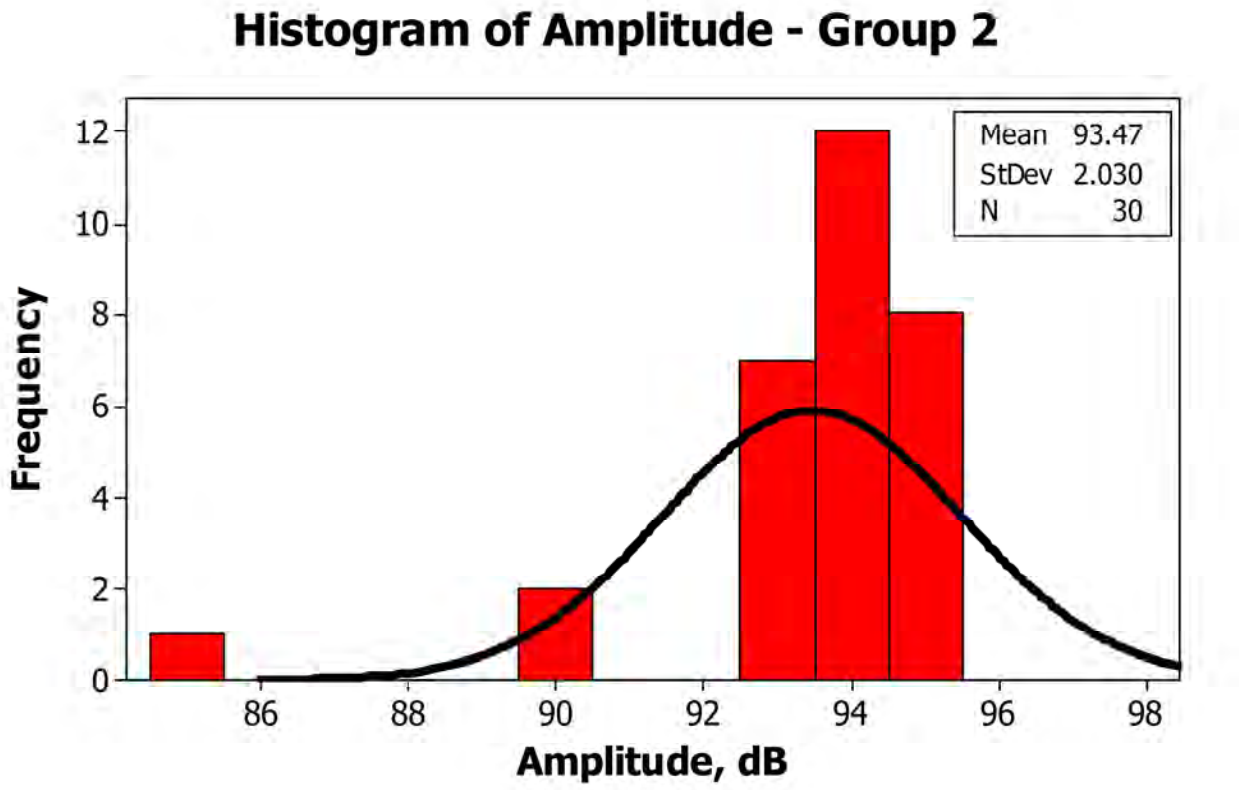

Figure 9. Distribution plot of AE hit amplitude for Group 2 (20 dB hardware preamp gain setting).

Identification of Characteristic AE Signal Features

Characteristic differences between AE signals for failures and non-failures can be seen from an analysis of collected AE data and distribution curves. There was a clear distinction between the amplitude of AE hits caused by friction/noise and fractures. A two-sample student's t-test showed that there was a statistically significant difference between the AE hit amplitudes of Group 1 and Group 2 ($p < 0.0005$, $\alpha = 0.05$). This parameter, AE hit amplitude, was selected as the primary criterion to pass or fail a part.

While the two-sample student's t-test showed a statistically significant difference between the average frequencies of non-failures (Group 1) and the failed parts (Group 2) ($p < 0.0005$, $\alpha = 0.05$), there was substantial overlap between the two distributions. Consequently, average frequency does not provide a distinct AE signal feature for separating defective and non-defective parts. Hence, a criterion based on average frequency was not recommended.

A two-sample student's t-test also showed a statistically significant difference between the AE hit energies of Group 1 and Group 2 ($p < 0.0005$, $\alpha = 0.05$). This parameter was therefore used to supplement the pass/fail criterion based on AE hit amplitude.

Selection of Pass/Fail Criteria

Pass/fail criteria were then selected based on the relative risks associated with making Type I and Type II errors. While neither error is desirable and both have potential economic impacts, the risks associated with accepting a defective part must be balanced with those of rejecting a non-defective part. The risk of making a Type II error was estimated by using the probability distributions of the Group 2 data. For example, using the histogram of AE amplitude, the probability of a hit falling below a selected threshold can be calculated. Because of the limitations (*i.e*. no information on the standard deviation of the data) associated with the "single value" distribution of the 40 dB preamp gain data, it is more appropriate to use the 20 dB preamp gain data. These data required additional treatment in order to be compared with non-failure data (collected with 40 dB gain). With the 20 dB preamp gain distribution (Figure 9) it was observed that the distribution amplitude centered around 93.5 ± 2.0 dB. Shifting the distribution 20 dB higher, as would be expected with the higher (40 dB) preamp gain setting, the mean became 113.5 dB. Possible variations in the data were compensated by selecting a more conservative mean value of 100 dB and a larger standard deviation value of 5.0. This new distribution was used to estimate the expected occurrence of failures below this particular amplitude. For example, assuming a mean amplitude for failures of 100 ± 5 dB, less than 3 parts per 10 million are expected to fall below a 75 dB threshold as shown in Figure 10. The probability of passing a bad part decreases with lower amplitude thresholds at the expense of increased probability of non-failure signals exceeding the threshold. Balancing these probabilities is critical to identifying appropriate pass/fail criteria.

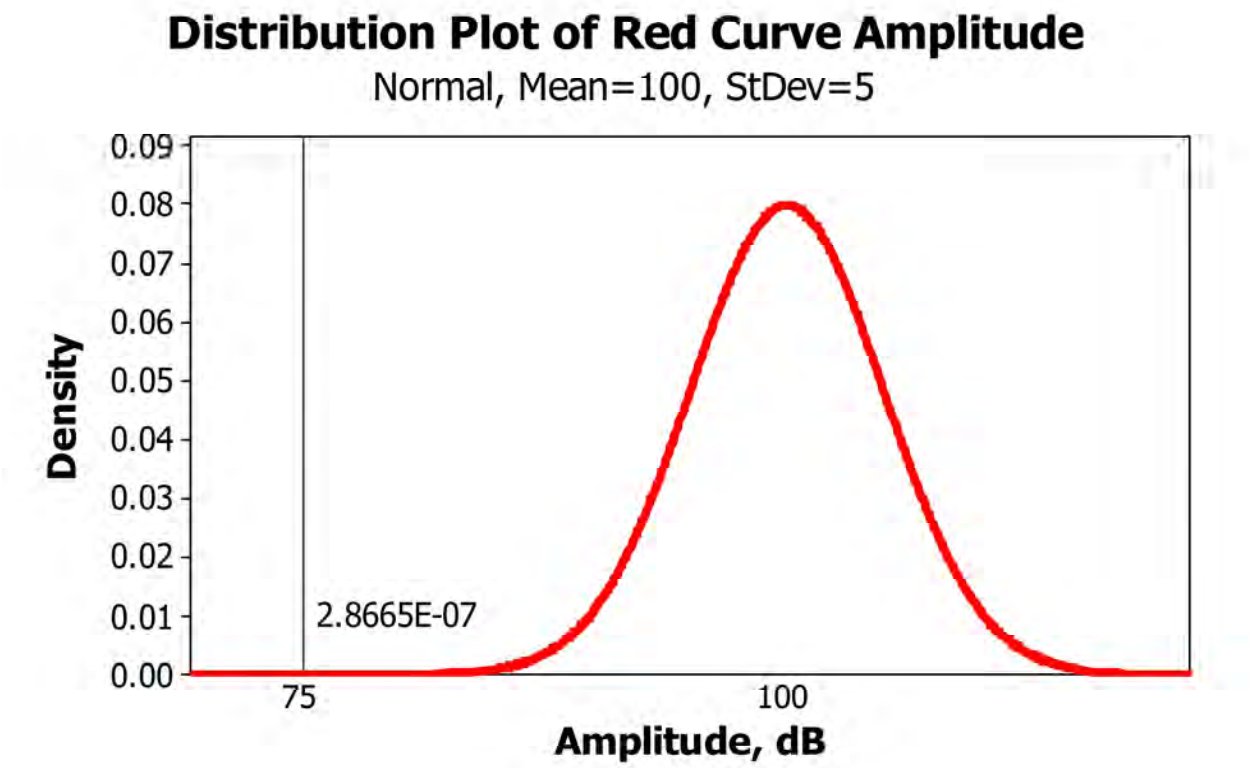

Figure 10. Probability distribution plot showing probability of 75 dB hit given the assumed red curve data.

Similarly, the non-failure distributions were used to estimate the risk of failing a good part (Type I error). Based on overall objectives, business, quality or otherwise, Type I and II errors were balanced to determine the appropriate pass/fail criteria. Further refinement of the AE monitoring process such as reduction in noise and friction signals may help reduce variability in distributions and further minimize the chance of making undesirable errors. Additionally, refinement of characteristic AE signal features may help to further develop the process. For example, while not fully evaluated due to constraints associated with the batch/lot processing of the implants and limitations in the AE software, derivatives of the AE hit energy such as cumulative energy and energy release rates may provide additional distinction between failure and non-failure signals. Using cumulative energy release, improved pass/fail criteria may be created for a test in which multiple hits stay below a given amplitude or energy count, yet indicate an accumulation of minor damage. Future refinement of this AE monitoring process may be used to more fully characterize failures/non-failures and further reduce the probabilities of making unwanted errors.

Implementation of AE Monitoring During Proof Testing

The use of AE monitoring during proof testing has many advantages and has been shown to be an effective method of identifying defects activated under an applied load. However, implementation of such a process required that several issues be considered and appropriately addressed. First was the efficacy of the proof test itself. It is not possible to universally identify the defects of a component due to the fact that existing flaws (*i.e.*, cracks, inclusions, voids, etc.) may only be activated in certain loading modes. A proof test is only effective if it closely

mirrors the type of loading that is expected during the service life of the implant.[23] In this study, for example, the proof test's primary loading mode was compression and was therefore not suitable for eliminating parts that might fail during tensile or torsional loading. Additional proof testing or inspection methods would be required to address other loading scenarios. Additionally, proof testing of ceramic materials must consider specific material properties. For example, ceramic materials which experience significant slow crack growth, unlike silicon nitride, may need special treatment, such as increased loading/unloading rates or load compensation.[20] Once an appropriate proof test was designed, the challenges of establishing AE monitoring could be addressed. In the case of silicon nitride intervertebral spinal spacers, the failure signals were shown to be distinct from background noise signals, though measures were taken to sufficiently reduce the latter to acceptable levels. Noise reduction and isolation allowed for the complete characterization of AE signals from which pass/fail criteria could be selected. Finally, risk analysis helped ensure that the selected criteria aligned with safety and business goals.

Summary and Conclusions

Having previously established an appropriate proof test method for silicon nitride intervertebral spinal spacers, monitoring of acoustic emissions during proof testing was developed, validated and implemented. AE monitoring during proof testing has been shown to be an effective and time-saving method (*i.e.*, near real-time feedback, with no secondary visual inspection) for identifying component failures during proof testing. Characterization of AE signal distributions was critical to differentiating between component failures and background noise and friction. Because AE monitoring is conducted in parallel with proof testing, operator feedback was almost immediate, leading to elimination of subsequent, time consuming secondary testing such as magnified visual and fluorescent penetrant inspections. It also removed the subjectivity of these secondary test methods such as operator skill level, operator vigilance, operator judgement, eye fatigue and defect detectability levels, among others. The use of AE monitoring during proof testing is expected to result in improved implant reliability and safety.

Acknowledgements

The authors would like to thank Brian Hedman, Jack Scothorne and Johnnatan M. Tenorio of the Amedica Corporation Quality Control Group for their assistance with proof testing and collection of AE data.

References

[1] B.S. Bal, M.N. Rahaman, Orthopedic Applications of Silicon Nitride Ceramics, Acta Biomater. 8 (2012) 2889–2898. doi:10.1016/j.actbio.2012.04.031.

[2] B.S. Bal, M. Rahaman, The Rationale for Silicon Nitride Bearings in Orthopaedic Applications, in: C. Sikalidis (Ed.), Adv. Ceram. - Electr. Magn. Ceram. Bioceram. Ceram. Environ., InTech, 2011: pp. 421–432. doi:10.5772/19381.

[3] B.S. Bal, A. Khandkar, R. Lakshminarayanan, I. Clarke, A.A. Hoffman, M.N. Rahaman, Fabrication and Testing of Silicon Nitride Bearings in Total Hip Arthroplasty, J.

Arthroplasty. 24 (2009) 110–116. doi:10.1016/j.arth.2008.01.300.

[4] A. Neumann, T. Reske, M. Held, K. Jahnke, C. Ragoß, H.R. Maier, Comparative Investigation of the Biocompatibility of Various Silicon Nitride Ceramic Qualities In Vitro, J. Mater. Sci. Mater. Med. 15 (2004) 1135–1140. doi:10.1023/B:JMSM.0000046396.14073.92.

[5] C.R. Howlett, E. McCartney, W. Ching, The Effect of Silicon Nitride Ceramic on Rabbit Skeletal Cells and Tissue: An In Vitro and In Vivo Investigation., Clin. Orthop. Relat. Res. 244 (1989) 293–304. doi:10.1097/00003086-198907000-00032.

[6] C.C. Guedes e Silva, B. König Jr., M.J. Carbonari, M. Yoshimoto, S. Allegrini Jr., J.C. Bressiani, Bone Growth Around Silicon Nitride Implants - An Evaluation by Scanning Electron Microscopy, Mater. Charact. 59 (2008) 1339–1341. doi:10.1016/j.matchar.2007.11.007.

[7] A. Neumann, C. Unkel, C. Werry, C.U. Herborn, H.R. Maier, C. Ragoß, et al., Prototype of a Silicon Nitride Ceramic-Based Miniplate Osteofixation System for the Midface, Otolaryngol. - Head Neck Surg. 134 (2006) 923–930. doi:10.1016/j.otohns.2006.01.022.

[8] M.C. Anderson, R. Olsen, Bone Ingrowth into Porous Silicon Nitride, J. Biomed. Mater. Res. Part A. 92A (2010) 1598–1605. doi:10.1002/jbm.a.32498.

[9] D.J. Gorth, S. Puckett, B. Ercan, T.J. Webster, M. Rahaman, B.S. Bal, Decreased Bacteria Activity on Si_3N_4 Surfaces Compared with PEEK or Titanium, Int. J. Nanomedicine. 7 (2012) 4829–4840. doi:10.2147/IJN.S35190.

[10] T.J. Webster, A.A. Patel, M.N. Rahaman, B.S. Bal, Anti-Infective and Osteointegration Properties of Silicon Nitride, Poly (Ether Ether Ketone), and Titanium Implants, Acta Biomater. 8 (2012) 4447–4454.

[11] M. Anderson, J. Bernero, D. Brodke, Medical Imaging Characteristics of Silicon Nitride Ceramic: A New Material for Spinal Arthroplasty Implants, in: 8th Annu. Spine Arthroplast. Soc. Glob. Symp. Motion Preserv. Technol., Miami, FL, 2008: p. 547.

[12] R.M. Taylor, J.P. Bernero, A.A. Patel, D.S. Brodke, A.C. Khandkar, Silicon Nitride - A New Material for Spinal Implants, J. Bone Jt. Surg. 92-Br (2010) 133.

[13] C.C. Guedes e Silva, O.Z. Higa, J.C. Bressiani, Cytotoxic Evaluation of Silicon Nitride-Based Ceramics, Mater. Sci. Eng. C. 24 (2004) 643–646. doi:10.1016/j.msec.2004.08.007.

[14] C.C. Sorrell, P.H. Hardcastle, R.K. Druitt, C.R. Howlett, E.R. McCartney, Results of 15-Year Clinical Study of Reaction Bonded Silicon Nitride Intervertebral Spacers, in: Proc. 7th World Biomater. Conf., 2004: p. 1872.

[15] J.E. Lincoln, Overview of the US FDA GMPs: Good Manufacturing Practice

(GMP)/Quality System (QS) Regulation (21 CFR Part 820), J. Valid. Technol. 18 (2012) 17.

[16] A.G. Evans, S.M. Wiederhorn, Proof Testing of Ceramic Materials - An Analytical Basis for Failure Prediction, Int. J. Fract. 10 (1974) 379–392. doi:10.1007/BF00962969.

[17] S.M. Wiederhorn, A.G. Evans, E.R. Fuller, H. Johnson, Application of Fracture Mechanics to Space-Shuttle Windows, J. Am. Ceram. Soc. 57 (1974) 319–323. doi:10.1111/j.1151-2916.1974.tb10910.x.

[18] S.M. Wiederhorn, A.G. Evans, D.E. Roberts, A Fracture Mechanics Study of the Skylab Windows, in: R.C. Bradt, D.P.H. Hasselman, F.F. Lange (Eds.), Fract. Mech. Ceram. Vol. 2 Microstruct. Mater. Appl., Springer US, Boston, MA, 1974: pp. 829–841. doi:10.1007/978-1-4615-7014-1.

[19] S.M. Wiederhorn, Reliability, Life Prediction and Proof Testing of Ceramics, in: Proc. Conf. "Ceramics High Perform. Appl., 1974.

[20] J.E. Ritter Jr, P.B. Oates, E.R. Fuller Jr, S.M. Wiederhorn, Proof Testing of Ceramics - Part 1 Experiment, J. Mater. Sci. 15 (1980) 2275–2281. doi:10.1007/BF00552317.

[21] E.R. Fuller Jr, S.M. Wiederhorn, J.E. Ritter Jr, P.B. Oates, Proof Testing of Ceramics - Part 2 Theory, J. Mater. Sci. 15 (1980) 2282–2295. doi:10.1007/BF00552318.

[22] H.G. Richter, G. Willmann, Reliability of Ceramic Components for Total Hip Endoprostheses, Br. Ceram. Trans. 98 (1999) 29–34. doi:10.1179/096797899680219.

[23] H. Kuhn, D. Medlin, eds., Mechanical Testing of Polymers and Ceramics, in: ASM Handbook, Vol. 8 Mech. Test. Eval., 2000: pp. 26–48. doi:10.1361/asmhba0003256.

[24] H. Fischer, W. Rentzsch, R. Marx, Elimination of Low-Quality Ceramic Posts by Proof Testing, Dent. Mater. 18 (2002) 570–5. http://www.ncbi.nlm.nih.gov/pubmed/12385897.

[25] M.J. O'Brien, A.R. de la Cruz, E.A. Nguyen, A Novel Proof Test for Silicon Nitride Balls, J. Am. Ceram. Soc. 94 (2011) 597–604. doi:10.1111/j.1551-2916.2010.04127.x.

[26] E.D. Megaw, Factors Affecting Visual Inspection Accuracy, Appl. Ergon. 10 (1979) 27–32. doi:10.1016/0003-6870(79)90006-1.

[27] C.G. Drury, J. Watson, Good Practices in Visual Inspection, Federal Aviation Administration/Office of Aviation Medicine, Washington DC, 2002.

[28] D.W. Richerson, Quality Assurance, in: Mod. Ceram. Eng., 2nd ed., Marcel Dekker, Inc., New York, 1992: pp. 620–647.

[29] K.R. Carunder, G.R. Hatfield, W.A. Ellingson, S.L. Dieckman, Nuclear Magnetic

Resonance Spectroscopy and Imaging of High-Performance Ceramics, in: N. Cheremisinoff (Ed.), Handb. Ceram. Compos. Vol. 2 Mech. Prop. Spec. Appl., Marcel Dekker, Inc., 1992: pp. 466–502.

[30] W.A. Ellingson, R.J. Visher, R.S. Lipanovich, C.M. Deemer, Optical NDE Methods for Ceramic Thermal Barrier Coatings, Mater. Eval. 64 (2006) 45–51.

[31] A.G. Evans, M. Linzer, Failure Prediction in Structural Ceramics Using Acoustic Emission, J. Am. Ceram. Soc. 56 (1973) 575–581. doi:10.1111/j.1151-2916.1973.tb12419.x.

[32] S. Wakayama, C. Ikeda, J. Ikeda, AE Monitoring of Microdamage During Proof Test of Bioceramics for Artificial Joints, J. Acoust. Emiss. 24 (2006) 228–233.

[33] C.B. Scruby, An Introduction to Acoustic Emission, J. Phys. E. 20 (1987) 946–953. doi:10.1088/0022-3735/20/8/001.

[34] G. Clark, J.F. Knott, Acoustic Emission and Ductile Crack Growth in Pressure-Vessel Steels, Met. Sci. 11 (1977) 531–536. doi:10.1179/030634577790432802.

[35] T. Ohira, Y.-H. Pao, Quantitative Characterization of Microcracking in A533B Steel by Acoustic Emission, Metall. Trans. A. 20 (1989) 1105–1114. doi:10.1007/BF02650145.

[36] H. Takahashi, M.A. Khan, M. Kikuchi, M. Suzuki, Acoustic-Emission Crack Monitoring in Fracture-Toughness Tests for AISI 4340 and SA533B Steels, Exp. Mech. 21 (1981) 89–99. doi:10.1007/BF02326364.

[37] M. Surgeon, E. Vanswijgenhoven, M. Wevers, O. Van Der Biest, Acoustic Emission During Tensile Testing of SiC-Fibre-Reinforced BMAS Glass-Ceramic Composites, Compos. Part A Appl. Sci. Manuf. 28 (1997) 473–480. doi:10.1016/S1359-835X(96)00147-9.

[38] Y.-H. Yu, J.-H. Choi, J.-H. Kweon, D.-H. Kim, A Study on the Failure Detection of Composite Materials Using an Acoustic Emission, Compos. Struct. 75 (2006) 163–169. doi:10.1016/j.compstruct.2006.04.070.

[39] G. Drummond, J.F. Watson, P.P. Acarnley, Acoustic Emission from Wire Ropes During Proof Load and Fatigue Testing, NDT&E Int. 40 (2007) 94–101. doi:10.1016/j.ndteint.2006.07.005.

[40] J.B. Wachtman, Highlights of Progress in the Science of Fracture of Ceramics and Glass, J. Am. Ceram. Soc. 57 (1974) 509–519. doi:10.1111/j.1151-2916.1974.tb10799.x.

[41] J.M. Carlyle, Acoustic Emission Testing the F-111, NDT Int. 22 (1989) 67–73. doi:10.1016/0308-9126(89)90859-6.

[42] J. Webster, I. Marinescu, R. Bennett, R. Lindsay, Acoustic Emission for Process Control and Monitoring of Surface Integrity During Grinding, CIRP Ann. - Manuf. Technol. 43 (1994) 299–304. doi:10.1016/S0007-8506(07)62218-5.

[43] D.E. Lee, I. Hwang, C.M.O. Valente, J.F.G. Oliveira, D.A. Dornfeld, Precision Manufacturing Process Monitoring with Acoustic Emission, Int. J. Mach. Tools Manuf. 46 (2006) 176–188. doi:10.1016/j.ijmachtools.2005.04.001.

[44] J. Barry, G. Byrne, D. Lennon, Observations on Chip Formation and Acoustic Emission in Machining Ti-6Al-4V Alloy, Int. J. Mach. Tools Manuf. 41 (2001) 1055–1070. doi:10.1016/S0890-6955(00)00096-1.

[45] L. Grad, J. Grum, I. Polajnar, J.M. Slabe, Feasibility Study of Acoustic Signals for On-Line Monitoring in Short Circuit Gas Metal Arc Welding, Int. J. Mach. Tools Manuf. 44 (2004) 555–561. doi:10.1016/j.ijmachtools.2003.10.016.

[46] H. V Ravindra, Y.G. Srinivasa, R. Krishnamurthy, Acoustic Emission for Tool Condition Monitoring in Metal Cutting, Wear. 212 (1997) 78–84. doi:10.1016/S0043-1648(97)00137-3.

[47] H.K. Tönshoff, M. Jung, S. Männel, W. Rietz, Using Acoustic Emission Signals for Monitoring of Production Processes, Ultrasonics. 37 (2000) 681–686. doi:10.1016/S0041-624X(00)00026-3.

[48] R.K. Miller, E. v K. Hill, P.O. Moore, eds., Acoustic Emission Testing, Volume 6, in: Nondestruct. Test. Handb., 3rd ed., American Society for Nondestructive Testing, Columbus, OH, 2005.

[49] I. Iturriza, F. Castro, M. Fuentes, Sinter and Sinter-HIP of Silicon Nitride Ceramics with Yttria and Alumina Additions, J. Mater. Sci. 24 (1989) 2047–2056. doi:10.1007/BF02385420.

[50] M.L. Villarraga, C.M. Ford, Applications of Bone Mechanics, in: S.C. Corwin (Ed.), Bone Mech. Handb., 2nd ed., Taylor & Francis Group, LLC, Boca Raton, FL, 2001: pp. 33–1–33–33.

[51] A.S. Przybyla, D. Skrzypiec, P. Pollintine, P. Dolan, M.A. Adams, Strength of the Cervical Spine in Compression and Bending, Spine (Phila. Pa. 1976). 32 (2007) 1612–1620.